

Electronic Supplementary Information (ESI[†])

Direct *versus* ligand-exchange synthesis of $[PtAg_{28}(BDT)_{12}(TPP)_4]^{4-}$ nanoclusters: effect of a single-atom dopant on the optoelectronic and chemical properties

Megalamanie S. Bootharaju,^a Sergey M. Kozlov,^a Zhen Cao,^a Moussab Harb,^a Manas R. Parida,^b Mohamed N. Hedhili,^c Omar F. Mohammed,^b Osman M. Bakr,*^b Luigi Cavallo,*^a and Jean-Marie Basset*^a

^aKAUST Catalysis Center, ^bKAUST Solar Center, and ^cImaging and Characterization Laboratory, King Abdullah University of Science and Technology (KAUST), Thuwal 23955-6900, Saudi Arabia

*To whom correspondence should be addressed. E-mail: jeanmarie.basset@kaust.edu.sa

luigi.cavallo@kaust.edu.sa

osman.bakr@kaust.edu.sa

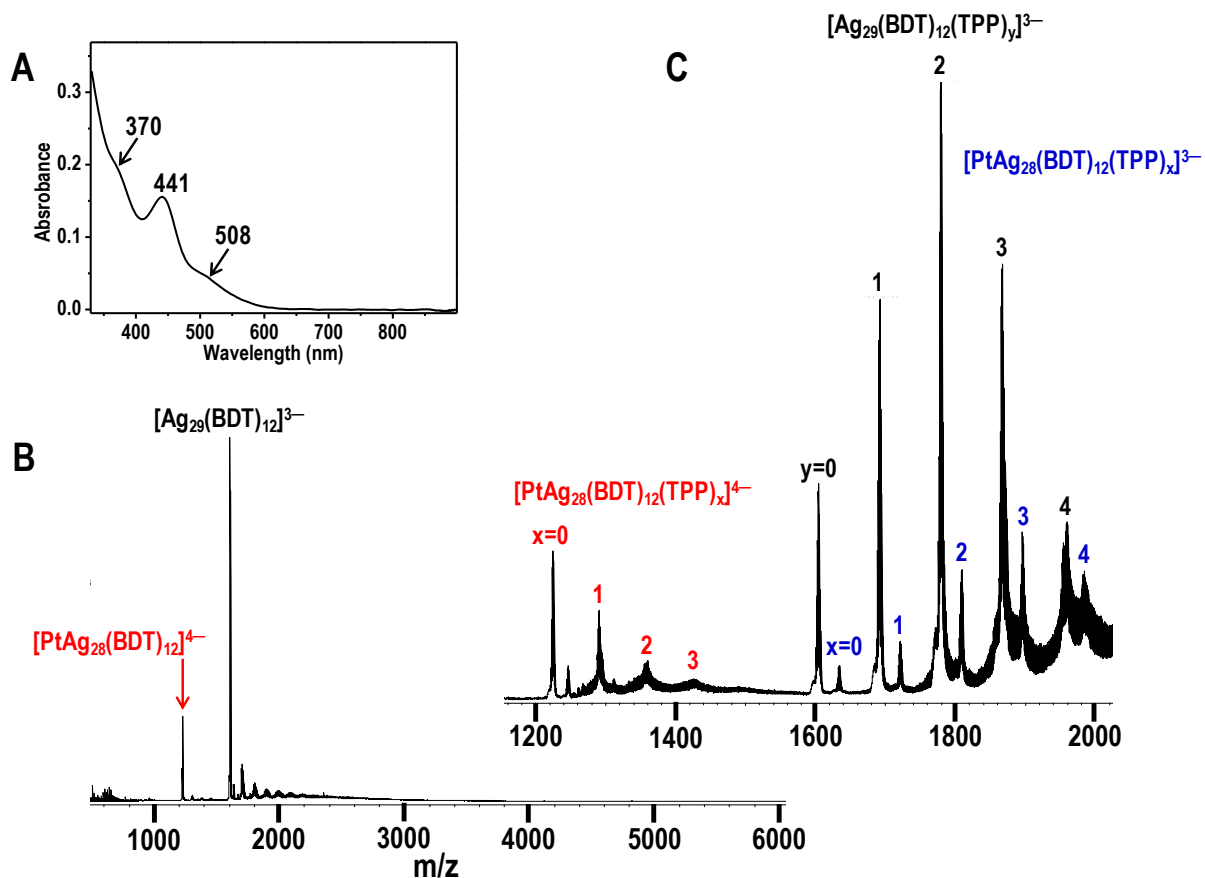


Fig. S1 (A) UV-vis absorption and (B) ESI MS (in negative-mode) spectra of the AgPt nanoclusters formed by borohydride reduction of Ag and Pt precursors in the presence of BDTH₂ and TPP ligands. (C) ESI MS of the same reaction product recorded under soft ionization conditions (low dry gas: 0.5–1.2 L/min) to obtain mass peaks with minimized fragmentation of TPP.

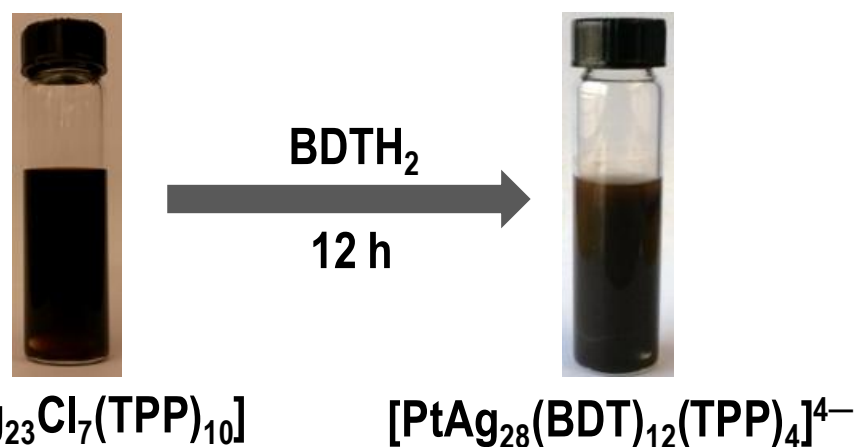


Fig. S2 Photographs showing LE transformation of $[\text{Pt}_2\text{Ag}_{23}\text{Cl}_7(\text{TPP})_{10}]$ NCs to $[\text{PtAg}_{28}(\text{BDT})_{12}(\text{TPP})_4]^{4-}$ NCs. A clear dark solution turned turbid after treatment with BDTH₂, indicating the occurrence of LE reaction.

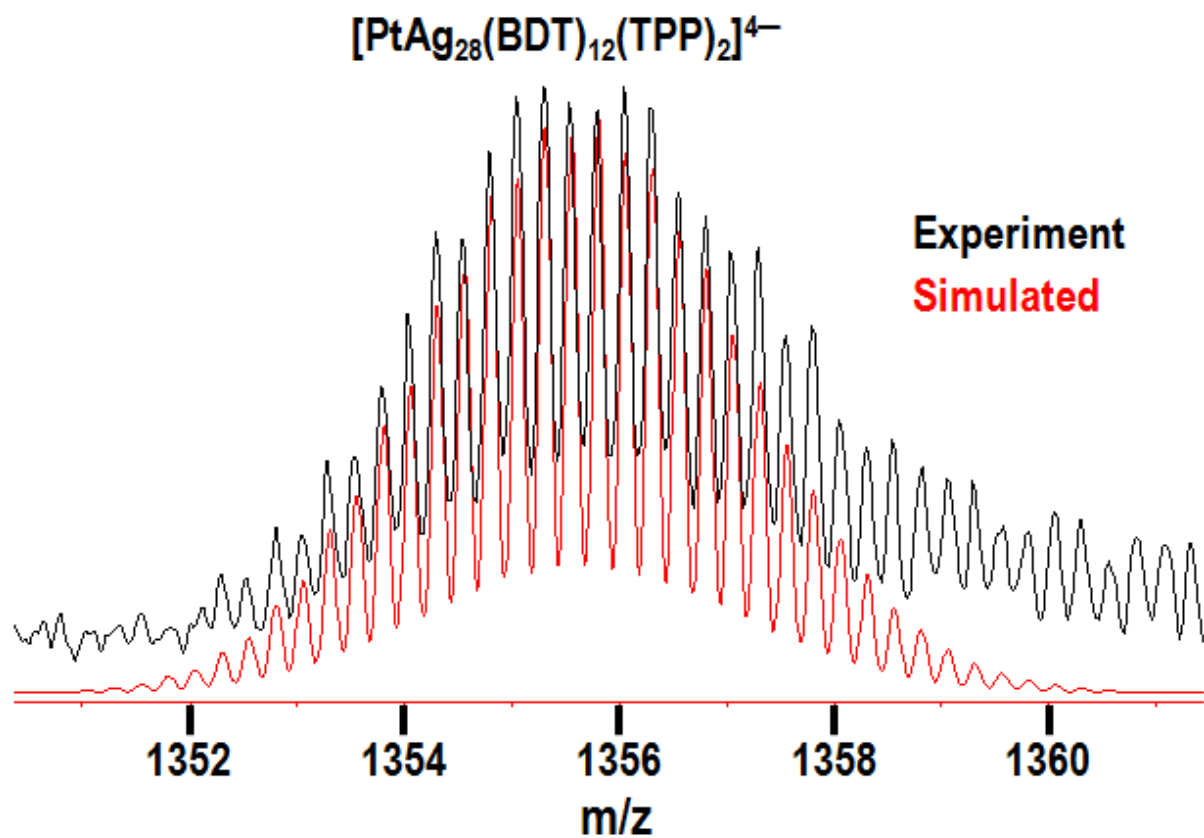


Fig. S3 Experimental ESI MS of the LE product $[\text{PtAg}_{28}(\text{BDT})_{12}(\text{TPP})_4]^{4-}$, where one of its fragments $[\text{PtAg}_{28}(\text{BDT})_{12}(\text{TPP})_2]^{4-}$ was compared with its simulated spectrum. The exact match between them confirms the formula assignment.

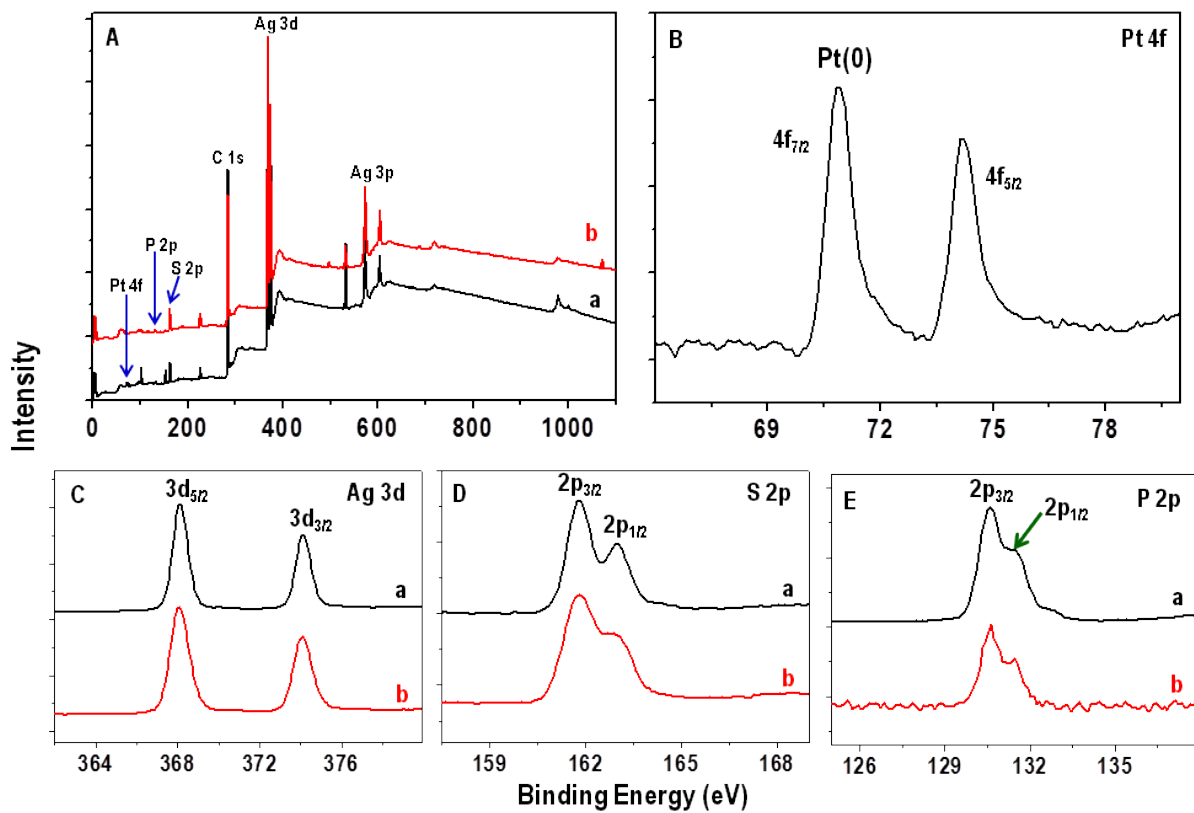


Fig. S4 (A-E) XPS survey, Pt 4f, Ag 3d, S 2p, and P 2p spectra, respectively of (a) $[\text{PtAg}_{28}(\text{BDT})_{12}(\text{TPP})_4]^{4-}$ and (b) $[\text{Ag}_{29}(\text{BDT})_{12}(\text{TPP})_4]^{3-}$ NCs.

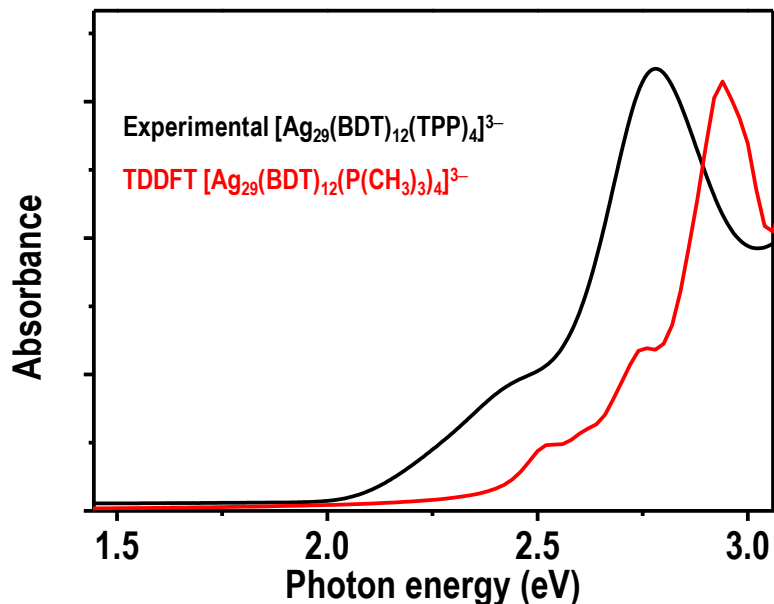


Fig. S5 Experimental absorption spectrum of $[\text{Ag}_{29}(\text{BDT})_{12}(\text{TPP})_4]^{3-}$ and TDDFT absorption spectrum of $[\text{Ag}_{29}(\text{BDT})_{12}(\text{P}(\text{CH}_3)_3)_4]^{3-}$ upon broadening by 0.05 eV Lorentzian.

Table S1. TDDFT calculated excitation energy, oscillator strength, and dominant (>10%) orbital contributions of main optical transitions (oscillator strength >0.02) of $[\text{PtAg}_{28}(\text{BDT})_{12}(\text{TPP})_4]^{4-}$ NCs.

Experimental feature	Transition	Oscillator strength (dimensionless)	Orbital contributions ^a
Shoulder of the high wavelength peak	2.575 eV (482 nm)	0.023	HOMOs→LUMOs (73%) HOMOs→LUMO+1 (19%)
Shoulder of the high wavelength peak	2.576 eV (481 nm)	0.024	HOMOs→LUMOs (73%) HOMOs→LUMO+1 (19%)
Shoulder of the high wavelength peak	2.581 eV (480 nm)	0.022	HOMOs→LUMOs (68%) HOMOs→LUMO+1 (24%)
High wavelength peak	2.653 eV (467 nm)	0.052	HOMOs→LUMO+1 (72%) HOMOs→LUMOs (19%)
High wavelength peak	2.662 eV (466 nm)	0.053	HOMOs→LUMO+1 (76%) HOMOs→LUMOs (13%)
High wavelength peak	2.663 eV (466 nm)	0.053	HOMOs→LUMO+1 (77%) HOMOs→LUMOs (13%)
Main peak	2.984 eV (415 nm)	0.164	HOMOs→LUMOs+2 (61%)
Main peak	2.984 eV (415 nm)	0.163	HOMOs→LUMOs+2 (61%)
Main peak	2.990 eV (415 nm)	0.163	HOMOs→LUMOs+2 (63%)

^a HOMOs and LUMOs include three orbitals with very similar energies and shapes and LUMOs+2 include two such orbitals.

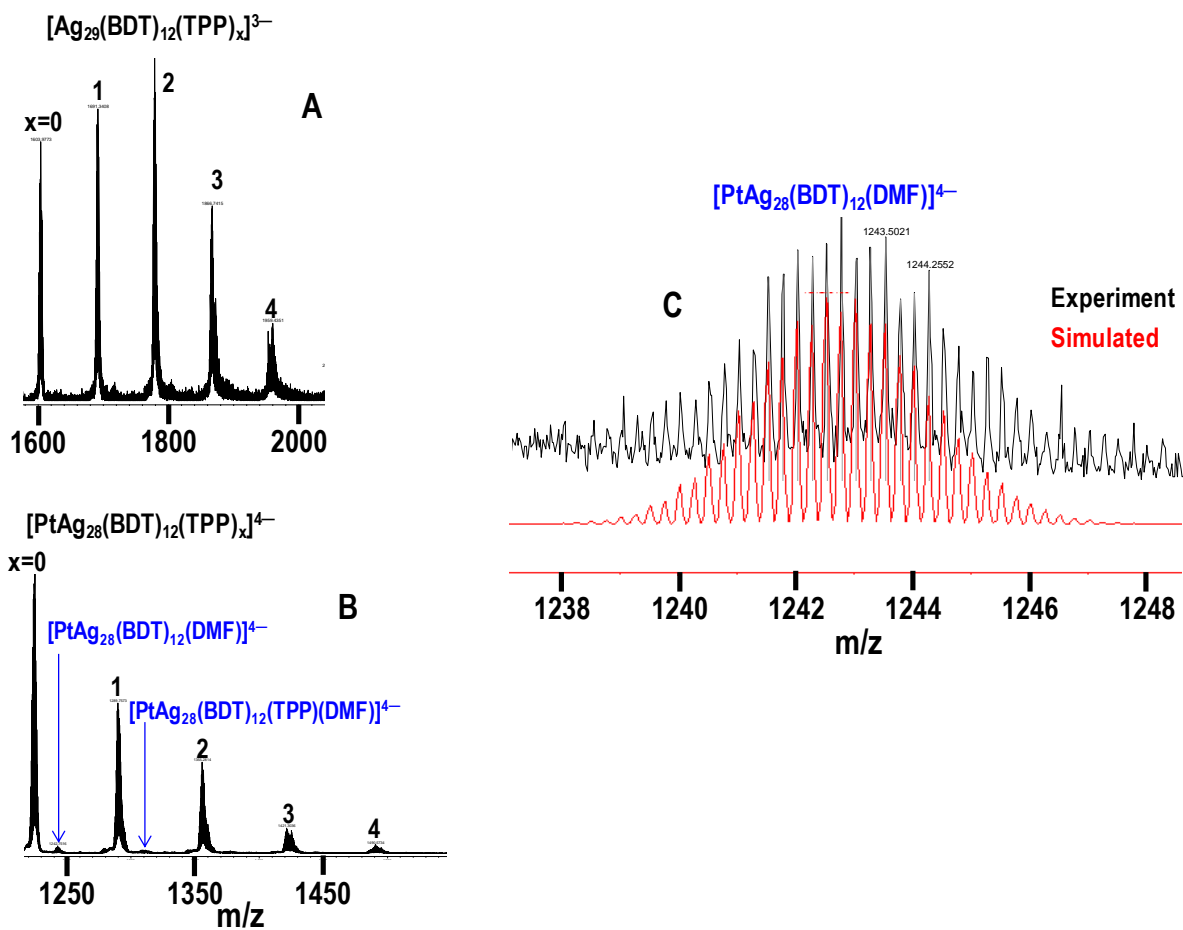


Fig. S6 ESI MS of (A) $[\text{Ag}_{29}(\text{BDT})_{12}(\text{TPP})_x]^{3-}$ and (B) $[\text{PtAg}_{28}(\text{BDT})_{12}(\text{TPP})_x]^{4-}$ NCs in DMF. The presence of DMF on the cluster surface is evident from B. (C) Comparison of experimental ESI MS of DMF-containing cluster peak of $[\text{PtAg}_{28}(\text{BDT})_{12}(\text{DMF})]^{4-}$ with its simulated spectrum. An exact match between them confirms the presence a DMF molecule on the cluster surface.

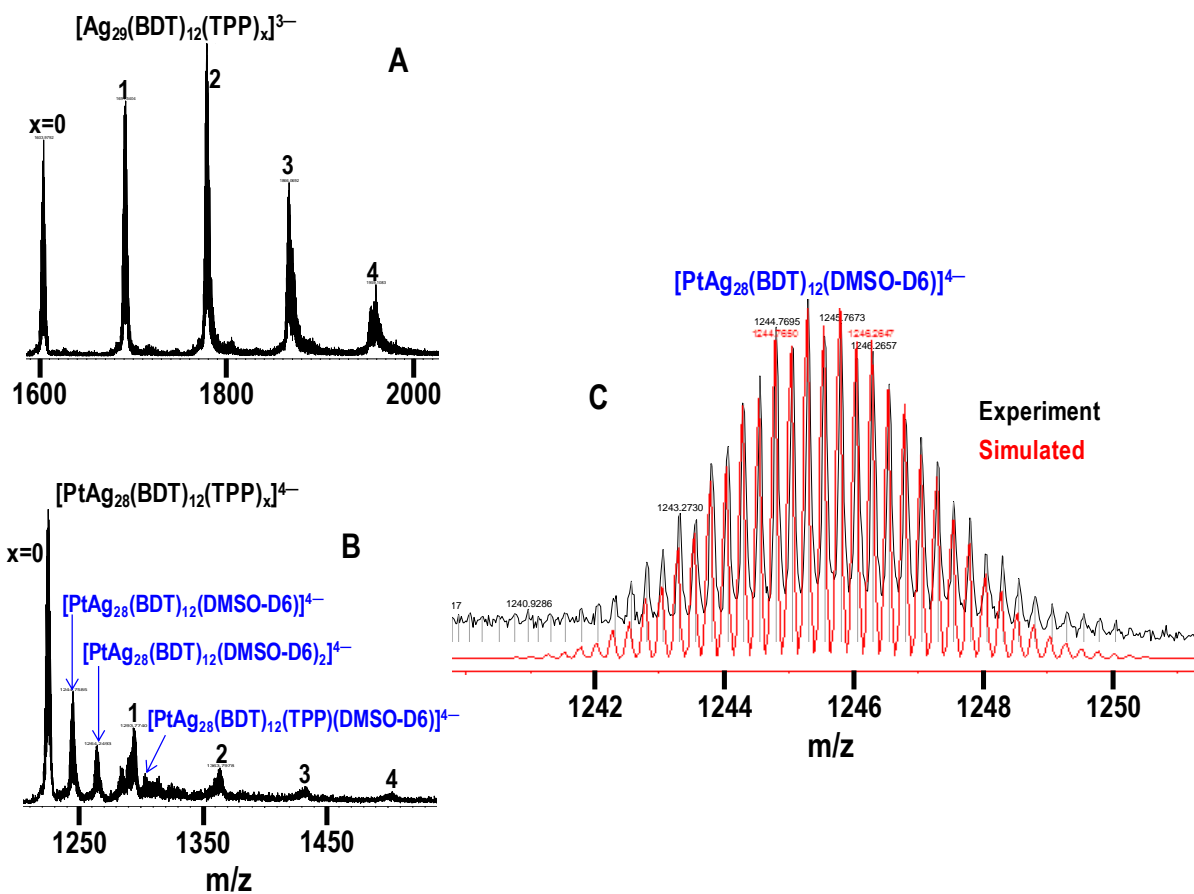


Fig. S7 ESI MS of (A) $[\text{Ag}_{29}(\text{BDT})_{12}(\text{TPP})_4]^{3-}$ and (B) $[\text{PtAg}_{28}(\text{BDT})_{12}(\text{TPP})_4]^{4-}$ NCs in DMSO-D6. The presence of DMSO-D6 molecules on the cluster surface is evident from B. (C) Comparison of experimental ESI MS of DMSO-D6-containing cluster peak of $[\text{PtAg}_{28}(\text{BDT})_{12}(\text{DMSO-D6})]^{4-}$ with its simulated spectrum. An exact match between them confirms the presence DMSO-D6 molecule on the cluster surface.

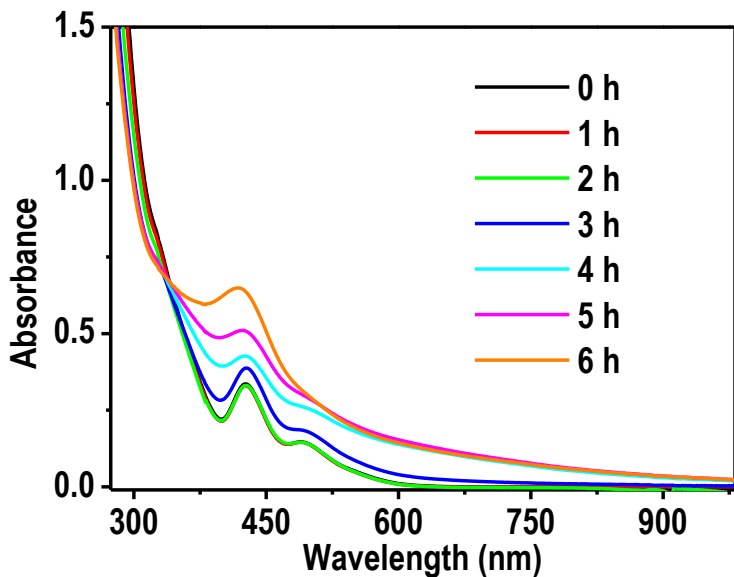


Fig. S8 Time-dependent UV-vis spectra of $[\text{PtAg}_{28}(\text{BDT})_{12}(\text{TPP})_4]^{4-}$ NCs in DMF heated at 80°C in air. The intact clusters features suggest their stability at least for 6 h.

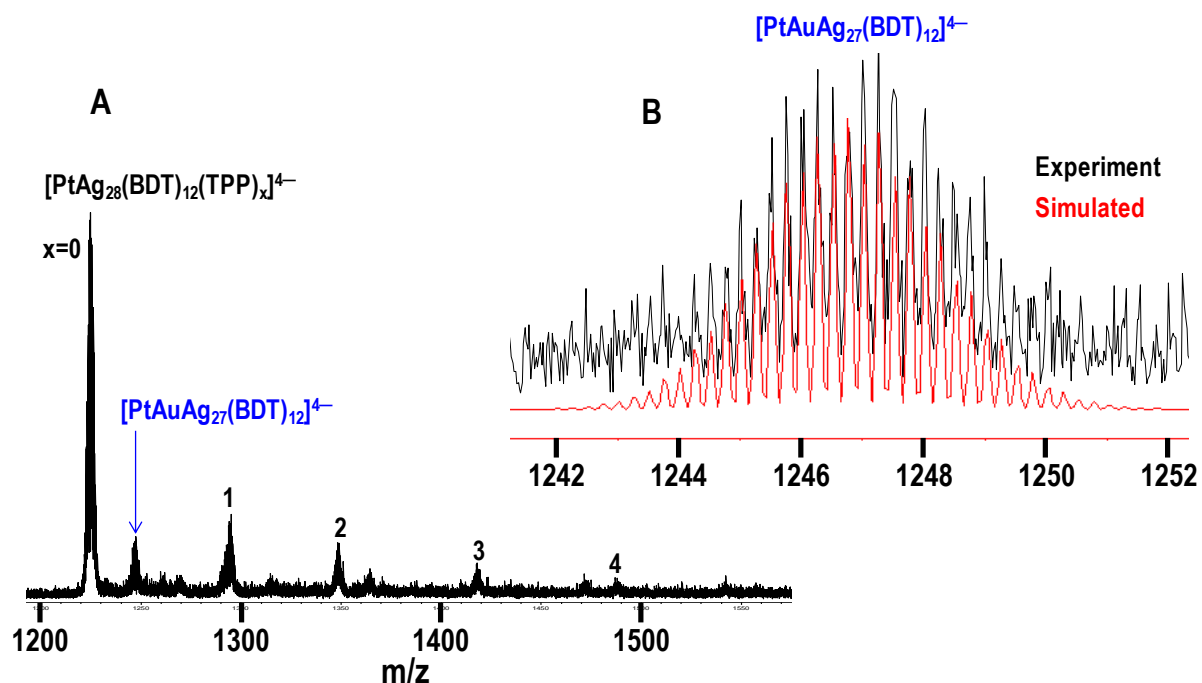


Fig. S9 (A) ESI MS of the metal-exchange product obtained by the reaction of $[\text{PtAg}_{28}(\text{BDT})_{12}(\text{TPP})_4]^{4-}$ with AuClTPP , showing an Au-exchange product of $[\text{PtAuAg}_{27}(\text{BDT})_{12}]^{4-}$ NC. (B) Comparison of experimental ESI MS of $[\text{PtAuAg}_{27}(\text{BDT})_{12}]^{4-}$ NC with its simulated spectrum. An exact match between them confirms the exchange of an Ag atom of PtAg_{28} clusters with an Au atom. The less intense peaks for TPP-intact mass species are due to high dry gas (2.0-3.0 L/min) during the mass spectral measurement.